ORIGINAL RESEARCH ARTICLE   **OPEN ACCESS**

MICROSTRUCTURE AND CORROSION CHARACTERISTICS OF CAST SILICON BRONZE IN AMMONIA ENVIRONMENT

Olatunde Sekunowo, Stephen Durowaye*, Oluwatoyin Bello

Department of Metallurgical and Materials Engineering, University of Lagos, Akoka, Lagos, Nigeria

*Corresponding author's email: durosteve02@yahoo.com

ABSTRACT

Refrigerating systems operating on either the open re-circulation or chilled water circuits are proned to corrosion attacks. Often, the ensued corrosion products foul and inhibit efficient heat transfer within the system causing leaks resulting in catastrophic failures. Thus, the imperative to search for a material that can be an effective substitute for the conventional copper pipe used in most refrigerating systems. In this study, the microstructure and corrosion susceptibility of cast silicon bronze in anhydrous ammonia environment was investigated. The silicon bronze was produced by sand casting with the silicon varied from 1-4 wt. %. An accelerated electrochemical polarisation technique was employed to simulate the corrosion behavior of the cast alloy. The results show relatively low corrosion susceptibility, 0.75 mm/yr of the alloy in anhydrous ammonia. This may be attributed to the silicon dioxide (SiO_2) passive film formed on the surface of the alloy. The effectiveness of the SiO_2 passive film increases as the wt. % of silicon addition increased. The potential for drastic reduction in maintenance cost and frequency of call-backs of refrigerating units is enhanced by the outcome of this study.

Keywords: Refrigeration, Silicon bronze, Anhydrous ammonia, Electrochemical polarisation

INTRODUCTION

The vapour compression refrigeration system is one of the many chilling cycles used for air-conditioning of buildings, automobiles, and large-scale chilling/frozen of foods, meats, and a host of other industrial services. Large vapour-compression refrigeration systems are also used in oil refineries, petrochemical and natural gas processing plants. Corrosion problems often occur in most if not all of these systems and plants [1]. The resulting corrosion products are known to inhibit heat transfer, fouling of the system, scaling, leakages and catastrophic system failures [2]. For example, the two major metals inside an absorption chiller components are made from ferrous (the shell) and cuprous (the heat transfer tubes) materials. Each of the metals reacts with oxygen hence, corrodes under varying conditions thereby complicating the technique for their protection against corrosion.

It is therefore imperative that investigations are carried out on materials used in absorption heating and refrigeration fluids to generate relevant data for its real time corrosion analysis. This is intended to aid the selection of a single material that can handle as many fluids as possible to prevent the pipe network from suffering debilitating corrosion. It has been established that pitting corrosion is the characteristic failure mode of copper pipes used in refrigerating system [3]. This often causes loss of refrigerant liquid, reduction in efficiency of the refrigerating system and environmental pollution [4]. Consequently, corrosion resistance has become the principal design criterion for piping materials employed in refrigerating systems [5]. Various options can be adopted in specifying which material is capable of providing adequate protection against catastrophic corrosion. This usually involves the use of a metal that provides the desired service life at the lowest cost. However, in a situation where a longer service life is required coupled with uncertainty regarding corrosion over time, the practice has always been either to modify the material design for example, by increasing the wall thickness or to use a better corrosion resistant alloy. Either of these approaches involves making provision for

corrosion allowance and the corrosion allowance commonly specified for copper alloys is 0.8 mm [6]. However, the challenge lies in the fact that corrosion allowances can only be safely used when corrosion rates can be predicted with a high degree of reliability.

Tremendous progress has been made in understanding the corrosion susceptibility of copper in different environments, being one of the high-entropy alloys [7]. However, to achieve significant reduction in the incidents of failure of refrigerating units due to corrosion, replacement of the conventional copper pipe with silicon bronze seems to be attractive. This optimism stems from the superior mechanical and corrosion passivation characteristics of silicon bronze compared to monolithic copper [8]. Silicon bronze is categorised into two based on the silicon content. The low silicon category contains 1.5 % Si used for heat exchanger tubes, marine, and industrial hardware, and fasteners while the high silicon category is used for chemical process equipment and marine propeller shafts with a maximum of 3 % Si. Both categories are known for their good casting characteristics, appealing surface finish, and superior corrosion resistant properties even when submerged in liquids and chemicals. They also exhibit good strength in conjunction with the self-lubricity of silicon for excellent bearing and load properties [9]. In the as-cast condition, the microstructures of copper-silicon alloys consist of copper-silicon solid solution with a silicide compound depending upon the silicon content and other alloying elements present. Silicon bronze has extremely oriented microstructure which consists of   silicon dendrites and tin eutectics in alpha copper matrix. The homogeneous distribution of these phases within the matrix tends to aid homogeneous distribution of corrosion products [10].

The development of hermitic compressors was in response to the huge maintenance cost on vapour compressors used in most household refrigerators and freezers [11]. However, the impact of the type of refrigerant used often exerts profound effect on the corrosion susceptibility of the pipes. For example, ammonia and ammonium compounds are substances associated with inducement of stress corrosion in copper alloys [12]. These compounds can be found virtually everywhere including but not limited to the atmosphere, water treatment chemicals, and air chilling circuit systems. This work investigates the corrosion behavior of cast silicon bronze in anhydrous ammonia and compares the data generated with a view to determine its suitability as capillary tube material in lieu of the conventional copper pipe commonly used in refrigeration systems.

MATERIALS AND METHODS

Materials

The two major materials (copper bars and ferrosilicon pellets) used in this study were sourced commercially whereas the corrosive medium, ammonia in anhydrous form was obtained from a registered chemical substances analysis laboratory in Nigeria. Pictures of the copper bars and ferrosilicon pellets are shown in Figure 1.

(a)   (b)

Figure 1. Experimental materials: (a) copper bars (b) ferrosilicon pellets

Melting and Casting

The copper bar was first weighed using a digital weighing scale based on specific charge calculations and was melted at 1200 ^{0}C in an open-pit furnace. On obtaining a sufficiently molten melt, fluid-slag was properly skimmed off the molten copper and proportionate amounts of ferrosilicon (1 wt. %) was added to produce the silicon bronze. The melt was homogenized for 30 seconds followed by manual stirring with steel rods for about 2 minutes. The remaining slag/impurities were finally skimmed prior to pouring the molten alloy into prepared sand moulds. The melting procedure was repeated for the next set of batches containing 2 wt. %, 3 wt. %, 4 wt. % Si whereas the control sample had no ferrosilicon added to it. The chemical composition of the 2 wt. % cast sample was determined using Bench Top Arc Spectrometer (Model 120971/06, Teledyne Leeman Labs, Hudson, NH) and is presented in Table 1.

Table 1. Chemical composition of the 2 wt. % cast silicon bronze

Element	Pb	Ni	Fe	Mn	Zn	Si	Cu
Wt. %	0.04	0.50	0.70	1.20	1.30	3.60	92.66

Corrosion Campaign and Electrochemical Measurements

The accelerated corrosion test coupons at ambient temperature were mechanically sectioned off the as-cast silicon bronze to 1 x 0.5 mm dimension and polished using 400, 600, 800 and 1,000 grades of emery papers. To avoid surface contamination, the polished samples were cleaned with acetone, washed with distilled water, dried in air and stored in desiccators. The potentiodynamic polarisation was performed at room temperature using AUTOLAB (Model: PGSTAT 204N, Metrohm, Netherlands) in a three-electrode cell setup. Silicon-bronze coupon embedded in resin with its square surface (0.5 mm^2) in the electrode was used as the working electrode; platinum as counter electrode, and saturated silver/silver chloride (SSC) was the reference electrode while anhydrous ammonia was used as the electrolyte. The steady state open circuit potential (OCP) was noted followed by potentiodynamic measurements made from -250 mV against OCP to +250 mV at a scan rate of 1.0 mVs^{-1}. The corrosion current density (J_{corr}), corrosion potential (E_{corr}), corrosion rate and polarisation resistance, (R_p) were determined from the Tafel plot (Figure 3). The other relevant data obtained from the electrochemical polarisation measurements are presented in Table 2 and also illustrated in Figure 3.

Hardness Test

Brinell hardness test was carried out on the samples according to ASTM E-10 standard. Each prepared sample was placed on a desk top machine by which a 10 mm diameter hardened steel ball indenter was pressed into the sample's surface while a load of 500 kg was applied for 10-15 seconds. With the aid of a low magnification microscope, measurement of the resulting round impression was made to ±005 mm accuracy. Two different diameters of the impression (indentation) at right angles were measured, and the mean diameter was used as basis for calculating the Brinell hardness number (BHN). The results are illustrated in Figure 2.

**Microstructural Characterisation**

The samples were mechanically sectioned into the appropriate sizes and the surfaces smoothened by using a silicon-carbide impregnated emery paper of 320 grits mounted on a rotary wheel. Successive grinding of specimens involved the use of finer emery papers of 400, 600, and 800 grits. Polishing of specimens to obtain mirror-like surfaces was done with 6 µm metadi-paste carefully applied to the specimens' surfaces to avoid overheating. The mirror-like surfaces were then washed under a running tap water and dried. Etching was done by swabbing sufficient amount and appropriate concentrations of nitric acid mixed with distilled water on the surfaces and then left for 20 seconds after which they were rinsed in deionized water, degreased, and dried. The specimens' microstructural features were then viewed under a scanning electron microscope (SEM) and the results presented in Figure 5-8.

RESULTS AND DISCUSSION

Hardness

The result of hardness test carried out on the as-cast silicon-bronze containing varied silicon addition is illustrated in Figure 2 at 5 % error. The control sample exhibited the highest hardness, 87.4 BHN whereas the value dropped significantly by 31.9 % (59.5 BHN) on the addition of 1 wt. % Si. However, the hardness value increases to 82.3 BHN at 2 wt. % Si addition and decreases progressively to 74.4 BHN and 61.7 BHN for the 3 wt.% Si and 4 wt. % Si additions respectively. The rather huge decrease in hardness at 1 wt.% Si addition might have stemmed from disorientation of the normal structural phases prevailent in copper resulting in a weak intergranular cohesion (Figure 6b). Further, addition of silicon up to 2 wt. % gave rise to the formation of an eutectic structure that is coherent with the copper matrix. This transformation must have significantly enhanced the interfacial cohesion between the phases present in the alloy hence, the increase in hardness. The addition of 3 wt.% Si and 4 wt.% Si however, increased the volume fractions of weak eutectic structure within the matrix giving rise to the continuous decrease in hardness within this range of silicon addition. From these observations, it appears that 2 wt. % Si addition in copper is the optimum limit of structure compactibility for inducement of better hardness in silicon-bronze. The alloy's hardness value of 82.3 BHN at 2 wt. % Si can be considered adequate for a material meant for structural applications, in particular when such material is meant to function under a relatively low temperature such as the case in refregerant fluid piping [13]. This level of hardness also has the potential for a relatively strain hardened-free deformation during extrusion of the alloy.
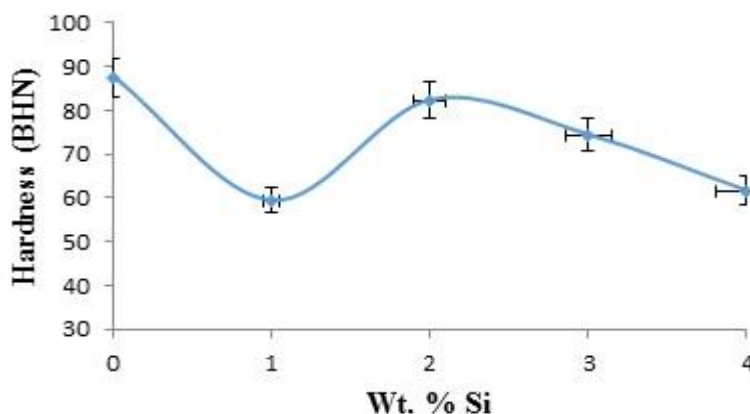
**Figure 2.** Hardness variation with silicon addition in copper bronze

Electrochemical Polarisation Behaviour

Table 2 shows the data generated during electrochemical polarisation of cast silicon bronze in anhydrous ammonia and the plot is shown in Figure 3. The corrosion current density (J_{corr}), and corrosion potential (E_{corr}) values were determined by the intersection of extrapolated anodic and cathodic Tafel lines. The corrosion current density and corrosion rate decrease drastically though varied with wt. % Si additions. The anodic Tafel slope decreases for all the scans from -0.7174 to -1.1348 V/dec, that of cathode increases from 0.1321 to 0.2242 V/dec with little variations. The corresponding anodic and cathodic Tafel values are -0.5897 and 0.2011 for the control (copper) sample. The immediate implication of these varying potentials regime between cathodic and anodic reactions indicates higher corrosion rate of copper compared with the cast silicon bronze. This submission is further reinforced by the corrosion potential (E_{corr}) values which decreases from -0.6313 to -0.7235 Obs (V) with varied weight percent of silicon. The values of the corroding current (I_{corr}) also decrease for all scans from 8.01 x 10^{-5}A to 1.03 x 10^{-5}A compared to 1.01 x 10^{-4} A for the control sample. The decreasing corrosion current (I_{corr}) exhibited by the cast silicon-bronze coupled with the same trend observed in the scans corrosion (E_{corr}) evidently show huge improvement in its corrosion resistance compared with copper. These outcomes may be attibuted to the presence of silicon that is known to exhibit no adverse chemical reactions in solution with most organic acids [8]. From Table 2, it is observed that the alloy polarisation resistance (R_p) increases as silicon composition in the alloy increases. This implies that the presence of silicon in the alloy serves to sustain the effectiveness of passive film formed on the surfaces of the alloy thereby lowering its corrosion rates.

Table 2. Polarisation resistance data obtained for cast silicon bronze containing varied silicon (wt. %) in anhydrous ammonia

Sample	ba (V/dec)	bc (V/dec)	E_{corr} Cal (V)	E_{corr} Obs (V)	J_{corr} (A/cm^2)	I_{corr} (A)	Polarisation Resistance (Rp)	Corrosion rate (mm/yr)
Control	-0.5897	0.2011	-0.62291	-0.6222	1.28E-04	1.0E-04	1319.4	1.4869
1 wt.. %Si	-0.7174	0.1321	-0.63242	-0.6313	1.02E-04	8.01E-05	1627.6	1.1856
2 wt. %Si	-2.8644	0.2717	-0.63946	-0.6308	7.96E-05	6.25E-05	1942.8	0.9246
3 wt. %Si	-0.8512	0.1608	-0.65782	-0.6561	4.99E-05	4.99E-05	2195.4	0.5803
4 wt. %Si	-1.1348	0.2242	-0.72201	-0.7235	1.31E-05	1.03E-05	6825.6	0.1525
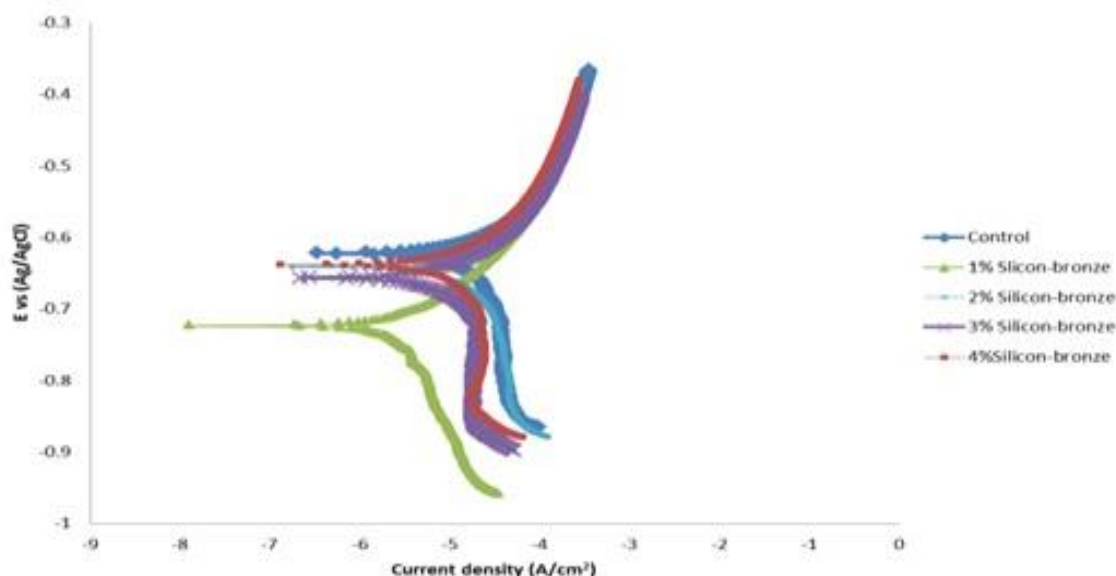
Figure 3. Potentiodynamic polarisation curves of cast silicon-bronze

Corrosion Rate

The corrosion rate demonstrated by the Cu-Si alloy at varied silicon addition in anhydrous ammonia is shown in Figure 4 with corrosion rate decreasing as the weight percent of silicon increases. The corrosion rate of copper being 1.487 mm/yr in the anhydrous ammonia environment is the highest compared to 1.186 mm/yr, 0.925 mm/yr, 0.580 mm/yr and 0.153 mm/yr respectively for 2 wt. % Si, 3 wt. % Si, and 4 wt. % Si additions. However, it is observed that the corrosion rate reduced by 20 % on the addition of just 1 wt.% Si. The reduction trend in corrosion rate continues on further addition of silicon. This behavior can be explained in the light of two possibilites; first, is the suppression of the highly motive copper ions, cu^+ and cu^{2+} by the rather inactive silicon which is not easily reducible [14]. The second possibility is that, silicon in combination with oxides/oxygen present in the system forms silicon monoxide (SiO_2) known to form an effective passive film on bronze surfaces which invariably gave rise to a significant reduction in the alloy's corrosion rate. It has been established that the addition of certain alloying element into some heat treatable metals serves the purposes of enhancing their corrosion resistance behaviour. For example, the reinforcement of aluminum with scandium reportedly gave rise to a significant reduction in corrosion rate in particular, the resistance to pitting corrosion [15]. It is evident from Figure 4 that as the silicon content increases, the amount and stability of SiO_2 passive film in the system increases thereby resulting in further reduction in corrosion rate.
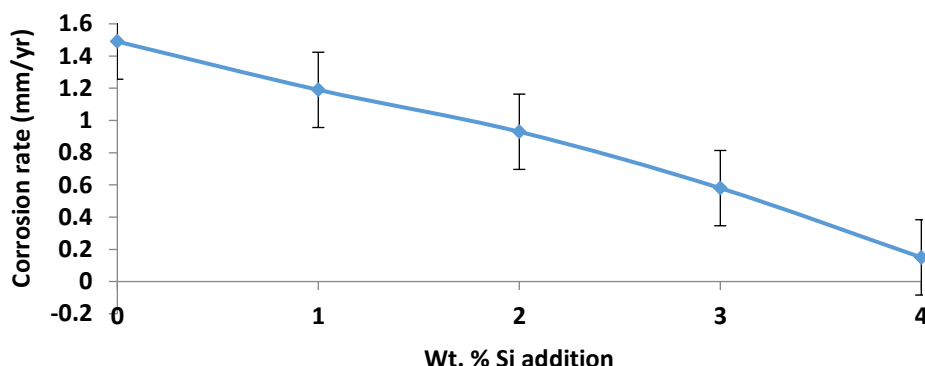
Figure 4. Effect of Silicon addition on corrosion rate of silicon-bronze in anhydrous ammonia

Microstructure

The cast silicon bronze specimens' microstructures before and after they have undergone corrosion simulations are analysed using a scanning electron microscope (SEM). The micrographs are presented in Figure 5-8. Prior to electrochemical simulation in the anhydrous ammonia environment (Figure 5a), the microstructure reveals a randomly oriented grains with coarse core and dendritic islands of inclusions which are not dispersed homogenously. However, on subjection to electrochemical reactions, a massive dissolution of the matrix is noticed (Figure 5b). The degradation rate of 1.487 mm/yr as obtained in this study appears massive resulting in gully-like erosion scenario. This may be attributed to the relatively soft copper matrix compared to the attacking power of corrosive specie (H^+) in the electrochemical system.

Figure 6a shows the presence of a relatively low volume fraction of a second-phase particles (Si) sparsely distributed within the copper matrix. After the electrochemical corrosion campaign (Figure 6b), attack on the matrix appears to occur on various crystallographic planes with attendant serious damage to the grain boundaries. This may not be unconnected with the issue of silicon particle grains coherency with the copper matrx. Generally, a weakly coherent second-phase particle cannot withstand the corroding attack of a highly motive cation like H^+ hence the type of microstucture that ensued. The microstructures developed on addition of 2 wt. % Si for the ascast and after electrochemical corrosion campaign are shown in Figure 7a and Figure 7b respectively. The dispersion of the second phase particles appears homogeneous within the copper matrix (Figure 7a) whereas, limited erosion of the matrix is observed on subjection of the alloy to electrochemical corrosion (Figure 7b). This accounts for the significant reduction in corrosion rate of the alloy compared with the control sample. On addition of 4 wt. % Si, a near saturated presence of the second phase develops within the matrix (Figure 8a). The pseudo-segregated structure's prevailence as seen in Fiure 8b significantly prevented access to both the grain boundaries and the matrix by the attacking corroding species within the system. Further, due to the relatively homogeneous structure developed in the alloy at 2 wt. % Si addition, the incident of corrosion induced by structure stratification is overcome and by extension, selective corrosion attack translating to pitting corrosion may have been prevented.
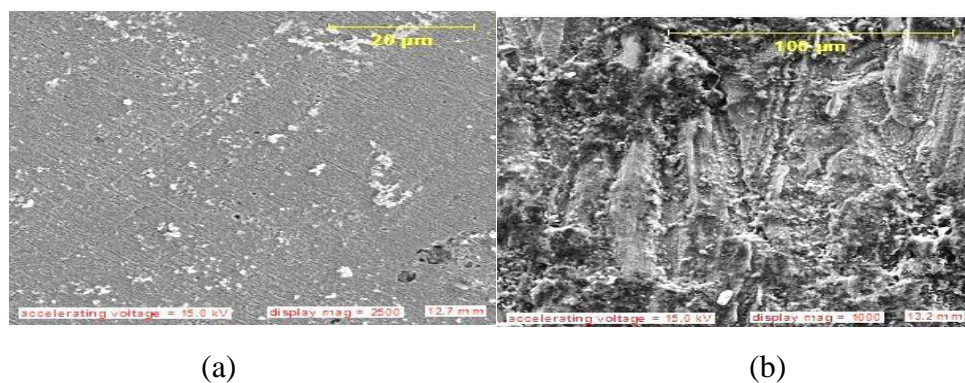
(a)   (b)
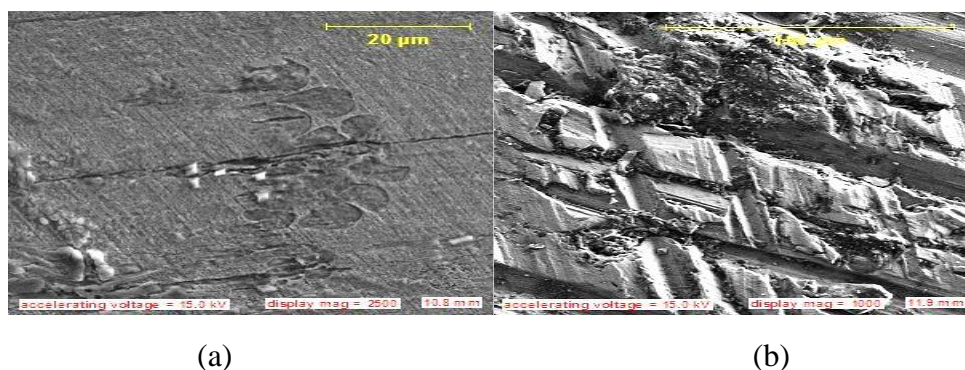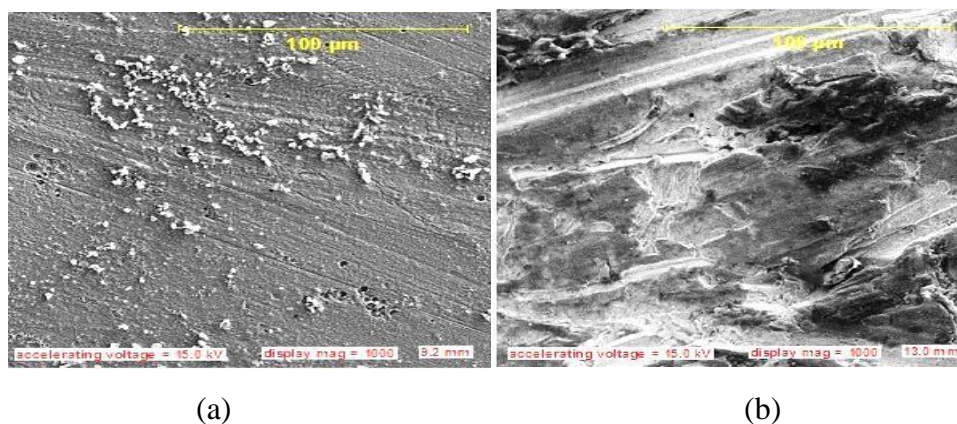
Figure 5. SEM micrographs of control samples (a) before and (b) after corrosion

(a)   (b)
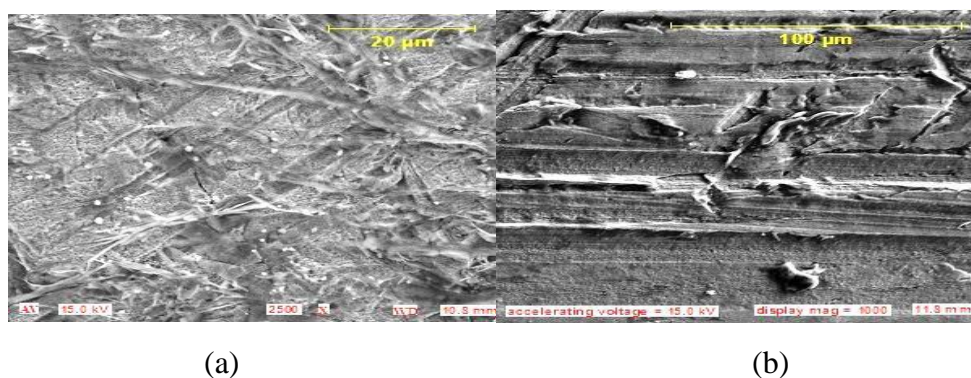
Figure 6. SEM micrographs of 1 wt. % Si addition (a) before and (b) after corrosion

(a)   (b)

Figure 7. SEM micrographs of 2 wt.% Si addition (a) before and (b) after corrosion

(a)   (b)

Figure 8. SEM micrographs of 4 wt. % Si addition (a) before and (b) after corrosion

CONCLUSIONS

Addition of varied amount of ferrosilicon to copper affects its corrosion susceptibility in anhydrous ammonia resulting in average corrosion rate reduction of 0.75 mm/yr per wt. % Si addition compared to 1.46 mm/yr exhibited by monolithic copper. Based on the experimental results, the following conclusions can be drawn:

i. The addition of a realatively low reactive element such as silicon confers significant potential for increase in corrosion resistance of silicon-bronze in anhydrous ammonia environment.

ii. Drastic reduction in corrosion susceptibility of silicon-bronze in anhydrous ammonia is due to the protective oxide film (SiO_2) formed on the alloy's surface.

iii. The level of hardness, 82.3 BHN developed in the alloy, the relatively low corrosion rate, 0.92 mm/yr and the desirable polarisation resistance of 1942.8 respectively at 2 wt.% Si addition suggest the optimum limit of silicon addition in silicon-bronze for enhanced corrosion behaviour in anhydrous ammonia.

REFERENCES

[1] Myer K, *Mechanical Engineers Handbook, Energy and Powe*r, 4th edition, Wiley Publishers Inc., New York, USA (2015), ISBN: 978-1-118-11899-3.

[2] Fakhen A, Heat Exchanger Efficiency, *Journal of Heat Transfer*, 129 (2007) 9, 1268-1276.

[3] Ananthanarayanan P S, *Basic Refrigeration and Air Conditioning*, McGraw-Hill Education, (2013), 96-108.

[4] Amey S & Majgaonkar M E, Controlling Corrosion in Marine Refrigeration Systems, *Journal of American Society of Heating, Refrigerating, and Airconditioning Engineers*, ASHRAE (2011), 50-58.

[5] Sahu G K, *Handbook of Piping Design*, (1998), 276-395.

[6]   NACE, *Calculation of corrosion allowance*, http://www.wermac.org/materials/corrosionallowance.html, March 2014.

[7]   Tang Z, Huang L, He W & Liaw P K, Aluminum Alloying Effects on Lattice Types, Microstructures and Mechanical Behavior of High-Entropy Alloys Systems, *Journal of Minerals, Metals & Materials Society (JOM)*, 65 (2013), 1848-1858.

[8]   Craig B D & Anderson D S, *Handbook on Corrosion Data: Technology and Engineering*, (1994), 405-407.

[9]   Anchor Bronze & Metals Inc., http://www.anchorbronze.com/c655 00.htm, August 2016.

[10]   Fabjan E S, Kosec T, Kuhar V & Legat A, Corrosion Stability of Different Bronzes in Simulated Urban Rain, *Materials and Technology*, 45 (2011) 6, 585-591.

[11]   Ohkawa T, Kumakara E, Higashi H, Sakitani K, Higuchi M, Taniwa H & Ozawa H, Development of Hermetic Swing Compressors for CO_2 Refrigerants, *International Compressor Engineering Conference*, Purdue University, http://www.docs.lib.purdue.edu/icec /1609, April 2002.

[12]   Agarwal D C, Effect of Ammonia Concentration on Environment-Assisted Failures in a Low-Nickel Copper Alloy, *Journal of Failure Analysis*, 3 (2003) 5, 58-68.

[13]   American Welding Society, *ISO 9001-2000 Standard*, htpp://www.brazing.com, June 2000.

[14]   Zhu X, Yu X, Li X, Wang P & Yang D, Quantification of Characteristic Parameters for the Dissociation Kinetics of Iron–Boron Pairs in Czochralski Silicon, *Scripta Materialia*, 64 (2011) 3, 217-220.

[15]   Ahmad Z, Properties and Application of Scandium-Reinforced Aluminum, *Journal of the Minerals, Metals & Materials Society (JOM)*, 55 (2003) 2, 35-39.